Reactive Gas Mach Stems

Roger A. Strehlow

Citation: Physics of Fluids **7**, 908 (1964); doi: 10.1063/1.1711305
View online: http://dx.doi.org/10.1063/1.1711305
View Table of Contents: http://scitation.aip.org/content/aip/journal/pof1/7/6?ver=pdfcov
Published by the AIP Publishing

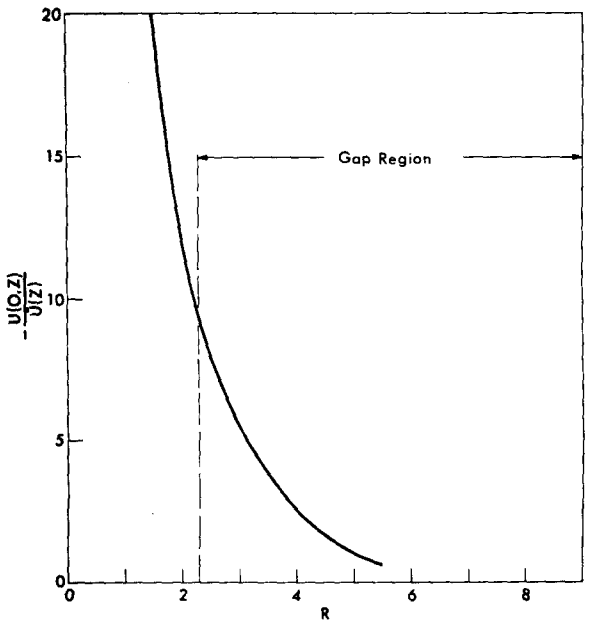

FIG. 1. Axial flow vs suction rate.

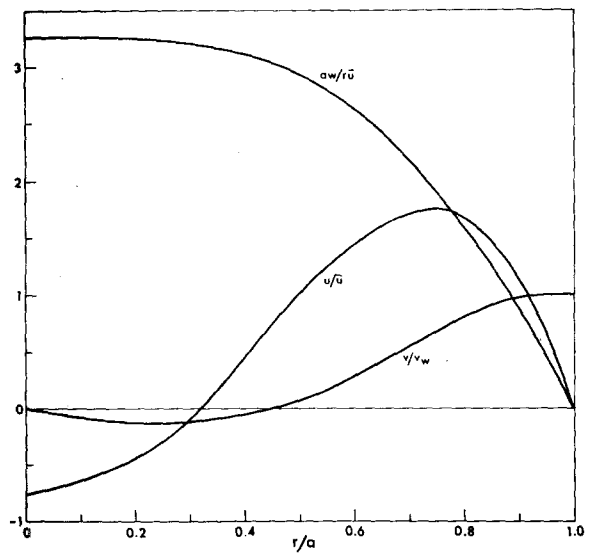

FIG. 2. Velocity profiles for $R = 5.29$.

The boundary conditions for a stationary pipe require that

$$f(0) = f'(1) = g(0) = g(1) = 0, \quad f(1) = \tfrac{1}{2}. \qquad (4)$$

Numerical solutions have been obtained for the system of equations (3) and (4) on an IBM 704 computer, using standard difference methods. Figure 1 shows a plot of the $u(0, z)/\bar{u}(z)$ as a function of R; we see that the fluid near the axis of the pipe moves in a direction opposite to that of the mean flow, and that this reversal becomes more and more pronounced as the suction goes to zero (as is to be expected, since the stationary pipe with impermeable

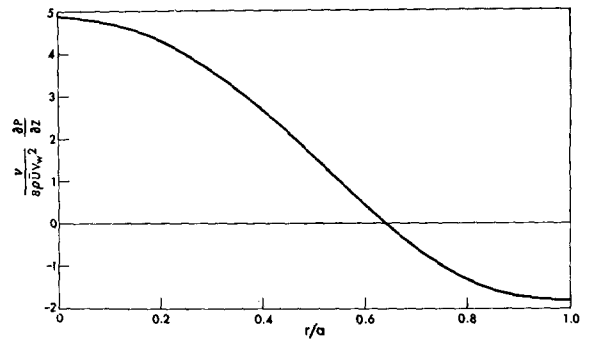

FIG. 3. Axial pressure gradient profile for $R = 5.29$.

walls allows no spiral flow solutions). The largest suction Reynolds number for which we have obtained solutions is $R = 5.29$, which is well within the gap region observed by Berman. Velocity and axial pressure gradient profiles for $R = 5.29$ are shown in Figs. 2 and 3. Not only the axial, but also the radial velocity reverses itself, and there is an annular region (from $r = 0.32a$ to $r = 0.64a$) in which the axial motion is in the direction of increasing pressure.

In conclusion, we may remark that spiral flows of the sort described here are also possible when fluid is injected through the pipe wall (negative R). The various profiles for this case are even more extreme; for example, $u(0, z)/\bar{u}(z)$ is 47 for $R = -2.1$, as compared to -11 for $R = +2.1$.

* This paper is based on work performed at the Oak Ridge Gaseous Diffusion Plant operated by Union Carbide Corporation for the U. S. Atomic Energy Commission.

[1] A. S. Berman, in *Proceedings of the Second International Conference on the Peaceful Uses of Atomic Energy* (United Nations, Geneva, 1959), p. 351.

[2] H. L. Weissberg, Phys. Fluids **2**, 510 (1959).

Reactive Gas Mach Stems

ROGER A. STREHLOW
Aeronautical and Astronautical Engineering Department, University of Illinois, Urbana, Illinois
(Received 10 February 1964)

THE observation of Mach stems produced in an exothermic reactive mixture have recently been reported by White and Cary[1] and White.[2] Their photographs clearly show that the slip-stream first separates unreacted gases, our u–u case, and at a later time separates reacted gas (behind the Mach stem) from unreacted gas (behind the reflected shock wave), our u–r case. Furthermore, as White[2] has indicated, the reaction zone behind the

reflected shock is preceded by another shock which lies parallel to and just ahead of the reaction zone.

This letter reports the results of triple shock interaction calculations for White's experimental composition assuming an ideal gas mixture and using thermodynamic data from the JANAF tables.[3] The calculations were performed using the Los Alamos HUG code[4] to obtain a table of unreacted or equilibrium shock properties for the incident or Mach stem shocks and then using the properties of the unreacted region behind the incident shock to calculate a table of unreacted reflected shock properties. A Fortran code was then used to calculate the (P, θ) balance criterion[5] at the slip-stream (see Fig. 1). Only ordinary (direct in Ref. 5) Mach stem solutions were considered. The calculation could be performed in this manner because u_1 was fixed and β was changed by changing w_1. Thus, the normal incident shock velocity remained constant and the thermodynamic properties in region 2 did not change with a change of β. The calculation was performed for both a u–u balance and a u–r balance at the slip-stream for values of β from the threshold value at large β to the lower β limit where the Mach stem shock becomes a normal shock wave.

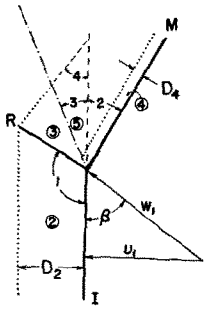

FIG. 1. Ordinary reactive Mach stem showing the two possible slip stream balances. M is the Mach stem shock, I the incident shock, and R the reflected shock. ··· reflected shock; — shock wave; -·- slip-stream. ③–⑤ balance is the u–r solution; ③–④ balance is the u–u solution.

The angles 1, 2, and 3 are directly determined from the balance criterion. The relative position of the adiabatic explosion waves following the incident and Mach stem shocks was determined by using the following expression

$$\frac{D_2}{D_4} = \frac{U_2 T_2 P_4}{U_4 T_4 P_2} : \exp\left[8635\left(\frac{1}{T_2} - \frac{1}{T_4}\right)\right],$$

where D is the distance behind the shock wave normal to the wave, U is the local flow velocity normal to the wave, T is the temperature in degrees Kelvin, and P is the local pressure. This expression was derived from Schott and Kinsey's[6] hydrogen–oxygen delay data and Kistiakowsky and Richards'[7] acetylene–oxygen delay data and applies reasonably well to the delay in the $4H_2 + 2O_2 + 4CO$ mixture White used (Fig. 6, Ref. 2). The angle of the reaction wave in region 3 (angle 4) was determined by computing the delay in that region at the slip-stream relative to that in region 2 at the reflected shock front and joining these end points with a straight line.

TABLE I. Reactive Mach stem structure.

(a) Photograph I (Fig. 1, Ref. 2)—$M_s = 4.8$, $P = 15$ mm, $4\,CO + 2\,O_2 + 4\,H_2$.

Quantity	Theoretical u–u Solution $\beta=50°$	$\beta=52°$	$\beta=54°$	Experimental values	Indicated β
∠1	124.35	121.23	117.75	122.0 ± 1°	51.5 ± .5°
∠2	33.93	31.06	28.29	30.5 ± 1°	52.4 ± .6°
∠3	23.73	23.65	23.53	23.5 ± 1°	53.9 ± 4.3°
∠4	48.90	38.84	31.07	37.0 ± 1°	52.4 ± .2°
D_2/D_4	7.52	6.18	5.13	5 $+2.3$ -1.3	54. ± 3°
					52.4 ± 1° av

(b) Photograph II (Ref. 8)—$M_s = 3.8$, $P = 15$ mm, $4\,CO + 2\,O_2 + 4\,H_2$.

	$\beta=52°$	$\beta=54°$	$\beta=56°$		
∠1	116.64	112.79	108.46	113.5 ± 3°	53.5 ± 1.2°
∠2	30.80	27.84	24.68	30.0 ± 3°	52.4 ± 3°
∠3	25.12	25.06	24.92	25° ± 3°	*OK*
∠4	62.26	50.44	39.91	63.5 ± 3°	51.7 ± .6°
D_2/D_4	10.3	8.0	6.2	4.3 $+3.7$ $-.8$	55° ± 4°
					53.0 ± 2° av

Table I is a comparison of the appropriate u–u calculation with two of White's experimental photographs. Notice that the experimentally indicated β shows good agreement for all the compared quantities. A satisfactory u–r comparison could not be obtained for these Mach stems. Thus it seems quite probable that the structure of the Mach stems White has photographed is determined by a balance criterion right at the triple point and the later slip-stream unbalance between regions 3 and 5 does not appreciably disturb this structure.

Interestingly enough, a calculation of the flow velocity in region 3 shows that it is indeed slightly supersonic relative to the reaction wave for these experimental Mach stem structures. Therefore, a reaction shock can exist just ahead of the reaction wave. However, this flow velocity is much less than the Chapman–Jouguet value for the conditions in region 3 and therefore the region behind the reaction wave cannot be a steady one-dimensional flow region.

The author would like to thank Dr. Garry L. Schott for many helpful discussions during the course of this work and Mr. Charles Hamilton for writing the Fortran code for the calculation. He would also like to thank Dr. D. R. White for supplying a glossy print of Fig. 1, Ref. 2 and an additional Mach stem photograph illustrating a different set of experimental conditions.

This work was performed at the Los Alamos Scientific Laboratory under the auspices of the U. S. Atomic Energy Commission.

[1] D. R. White and K. H. Cary, Phys. Fluids **6**, 749 (1963).
[2] D. R. White, Phys. Fluids **6**, 1011 (1963).
[3] *JANAF Interim Thermochemical Tables* (Dow Chemical Company, Midland, Michigan, 1960).
[4] P. F. Bird, R. E. Duff, and G. L. Schott, Los Alamos Scientific Laboratory Report LA 2980, 1964.
[5] R. Courant and K. O. Friedrichs, *Supersonic Flow and Shock Waves* (Interscience Publishers, Inc., New York, 1948), pp. 331–350.
[6] G. L. Schott and J. L. Kinsey, J. Chem. Phys. **29**, 1177 (1958).
[7] G. B. Kistiakowsky and L. W. Richards, J. Chem. Phys. **36**, 1707 (1963).
[8] D. R. White (private communication).

Dyson Equation Technique in Nonequilibrium Statistical Mechanics

G. KALMAN*
Service de Physique des Plasmas, Faculté des Sciences, Université de Paris, Orsay (Seine et Oise), France
(Received 11 October 1963; revised manuscript received 12 February 1964)

THE technique of the Dyson equation is an everyday tool in quantum mechanical perturbation calculations for the summation of a subclass of an infinite series of diagrams. In the formal solution of the Liouville equation[1] one encounters graphs of the same character which again represent a certain term in a given perturbation expansion. In the derivation of a kinetic equation[2] a subclass of such diagrams is selected out, an infinite sum of which contributes to a kinetic equation in some desired approximation. It is the purpose of the present note to point out that the technique of the Dyson equation can be applied for such a summation procedure as well and the cumbersome direct enumeration and summation of diagrams can easily be circumvented.

We use the original Prigogine–Balescu-diagram technique with some slight modification that is expedient in the present context. In addition to the horizontal lines representing the dynamical processes, we employ graphical symbols for the distribution functions[3] themselves. A circle (∘) is used to stand for the initial value of F, $F(\mathbf{k}, \mathbf{v}; t = 0)$ and a full circle (•) for $F(\mathbf{k}, \omega; \mathbf{v})$; similarly

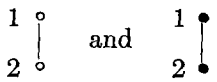

are associated with $\mathcal{G}(\mathbf{k}_1\mathbf{k}_2, \mathbf{v}_1\mathbf{v}_2; t = 0)$ and $\mathcal{G}(\mathbf{k}_1\mathbf{k}_2, \omega, \mathbf{v}_1\mathbf{v}_2)$, respectively. It is evident how similar symbols can be introduced for higher correlations, but they are not used here. 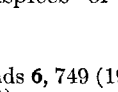 (or ∘ if $k = 0$) and

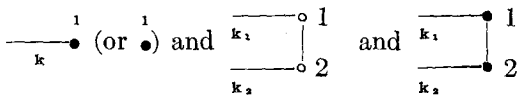

can be regarded as the unperturbed and perturbed propagators for F and $\mathcal{G}$, respectively.

By an obvious generalization of the rules pertaining to the usual open-circle diagrams, one finds the following prescription for the evaluation of the full-circle diagrams: If in a state (vertical cross section) one encounters a line terminating in a full circle, such line is to be associated with $F(\mathbf{k}, \omega, \mathbf{v})$; similarly a pair of lines terminating in a full dumbbell is to be associated with $\mathcal{G}(\mathbf{k}_1\mathbf{k}_2, \omega, \mathbf{v}_1\mathbf{v}_2)$. The total contribution of the state is the convolution product (with respect to ω) of all the individual factors represented by each line or pair of lines.

We elucidate the application of the present technique through some examples.

1. Vlasov equation. The Vlasov-equation is obtained if all diagrams of order $(e^2n)^m (m > 0)$ are retained. The corresponding diagrams are[2]

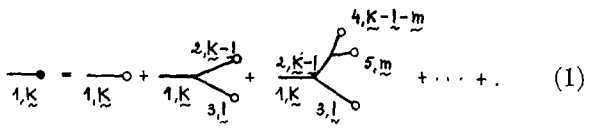

(1)

The mathematical expression represented by such graphs is well known. It is now obvious that the infinite series of graphs can be replaced by the following Dyson equation

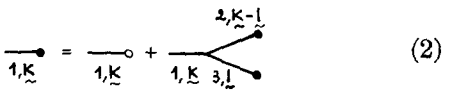

(2)

since (1) is generated by the iterative solution of (2). In view of the previously given rules, (2) is evidently the Vlasov equation.

2. Fokker–Planck equation. One arrives at the homogeneous Fokker–Planck equation by summing all graphs of the order $e^2(e^2t)^m$.[4] These are the connected and semiconnected circles. One easily convinces oneself that such a series of diagrams is the iterative solution of the Dyson equation

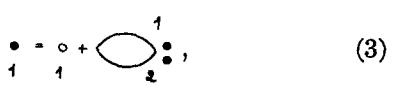

(3)

which, in turn, is the homogeneous Fokker–Planck equation.

3. Equation of evolution for $\mathcal{G}(k)$ in a plasma. For this case contributions of the order $e^2(e^2n)^m(e^2t)^{m'}$ are retained. The relevant diagrams are